



This is a repository copy of *Assessment criteria for optimal sensor placement for a structural health monitoring system*.

White Rose Research Online URL for this paper:

<https://eprints.whiterose.ac.uk/190292/>

Version: Accepted Version

Proceedings Paper:

Wang, T. orcid.org/0000-0002-1271-2641, Wagg, D.J., Worden, K. et al. (1 more author) (2022) Assessment criteria for optimal sensor placement for a structural health monitoring system. In: Farhangdoust, S., Guemes, A. and Chang, F.-K., (eds.) Structural Health Monitoring 2021 : Proceedings of the Thirteenth International Workshop on Structural Health Monitoring Stanford University, March 15-17 2022 (formerly December 7-9, 2021). IWSHM 2021 - 13th International Workshop on Structural Health Monitoring, 15-17 Mar 2022, Stanford University, CA, USA. DEStech Publications, Inc. , Lancaster, PA, USA , pp. 365-375. ISBN 9781605956879

This article appeared in its original form in the International Workshop on Structural Health Monitoring, 2021. Lancaster, PA: DEStech Publications, Inc.

Reuse

Items deposited in White Rose Research Online are protected by copyright, with all rights reserved unless indicated otherwise. They may be downloaded and/or printed for private study, or other acts as permitted by national copyright laws. The publisher or other rights holders may allow further reproduction and re-use of the full text version. This is indicated by the licence information on the White Rose Research Online record for the item.

Takedown

If you consider content in White Rose Research Online to be in breach of UK law, please notify us by emailing eprints@whiterose.ac.uk including the URL of the record and the reason for the withdrawal request.



eprints@whiterose.ac.uk
<https://eprints.whiterose.ac.uk/>

Title: Assessment criteria for optimal sensor placement for a structural health monitoring system

Authors : Tingna Wang
David J. Wagg
Keith Worden
Robert J. Barthorpe

ABSTRACT

Machine learning algorithms have been extensively used to implement structural health monitoring (SHM) systems to detect the occurrence of damage within a structure. To obtain the most effective data for SHM decision making, it is desirable to perform sensor placement optimisation (SPO), with a particular focus on damage identification. However, comparatively little attention has been paid to systematic assessment criteria appropriate to the design of a sensor system for SHM. This paper focusses on studying the evaluation criteria at different stages of a sensor-system design process, ranging from the measurement of linear associations to the detailed evaluation of the overall probability of correct classification. The effects of the investigated criteria are demonstrated using a physics-based model with uncertain parameters related to material properties. Predictions of the dynamic response of the structure in different states of interest are used to derive features.

INTRODUCTION

At the design stage of a structural health monitoring (SHM) system, a physics-based model can be used to provide predictions of dynamic response of structure in the different states of interest. To make the predictions from a model more reliable, approaches incorporating the uncertainties of input parameters into model simulation have received a great deal of interest in the research literature [1]. The most intuitive way to implement uncertainty propagation is via Monte Carlo sampling [2]. However, for large-scale models, the computational cost of the process can be prohibitive. Some surrogate modelling methods have been developed to overcome this limit, such as the polynomial chaos expansion, Gaussian process regression (also referred to as Kriging) and neural networks [3–5].

Based on the above research, some studies on sensor placement optimisation (SPO) technologies by using features derived from model predictions has been carried out. Gu-ratzsch & Mahadevan (2010) proposed a probabilistic finite element model analysis to

Tingna Wang, David J. Wagg, Keith Worden, Robert J. Barthorpe, Dynamics Research Group, Department of Mechanical Engineering, University of Sheffield, Mappin Street, Sheffield, S1 3JD, UK. Email: twang71@sheffield.ac.uk

provide measurements for the subsequent SPO process [6]. The spatial and temporal distribution of model parameters was considered via a random process or random field. Monte Carlo sampling was adopted to transfer the uncertainty of input variables to outputs. Castro-Triguero et al. (2013), also used Monte Carlo simulation to realise the propagation of parametric uncertainties, but focussed on investigating the influence of these uncertainties on the SPO methodologies based on the Fisher information matrix and energy matrix rank [7]. Eshghi et al. (2019), developed a reliability-based method to optimise the sensor network design, considering the uncertainty of structural geometry and input force amplitude [8]. Kriging combined with Latin hypercube sampling was applied to reduce the computational cost of generating training and testing data for cases with different health states, sensor locations and sensor sizes. It can be found that the focus of current research on sensor system design is on how to consider the model uncertainties in the optimisation and to find the influence of these uncertainties.

Since the study of system assessment criteria for the design process has received little attention in the reviewed literature, this paper will endeavour to address this gap by introducing a hierarchical evaluation system to improve the optimisation design of the SHM sensor network. The key novelty of this paper is to present a systematic process for SHM sensor optimisation design and put forward corresponding evaluation indicators suitable for different stages of the process. It will be shown that this method can support decision making with respect to number, type and locations of sensors.

The structure of this paper is as follows. Section 2 introduces the framework of assessment criteria. Section 3 describes the numerical model of a rectangular plate to provide data for the case study. The results for the case study are then shown and discussed in Section 4. Finally, conclusions are presented in Section 5.

ASSESSMENT CRITERIA

There are key distinctions between the cost functions used for different stages of a sensor system design. When the task is to select an optimal sensor combination from a large number of candidates, the cost functions need to be quick to evaluate to enable efficient optimisation and it may be acceptable for them to be abstracted from the main aim of the system to some extent. For the final system evaluation, to decide the number of sensors and the sensor type, the priority is to make the most accurate evaluation possible of how the system will perform in practice.

Stage 1 - optimal sensor combination

The task at hand is achieving optimal spatial deployment of sensors for binary or multiclass classification. In this paper, the *multiple correlation coefficient* (MCC) is investigated as a possible early-stage assessment criterion, which is designed to measure the maximal linear association between a set of independent variables and a dependent variable [9]. Here, the N observations with n independent variables are represented by a matrix \mathbf{X} of dimension $N \times n$. An $N \times 1$ vector of labels associated with each observation is represented by \mathbf{y} . The essence of the MCC analysis of \mathbf{X} and \mathbf{y} is to find a projection direction of \mathbf{X} that can maximise the linear correlation between \mathbf{y} and the

projected \mathbf{X} , which can be realised by,

$$R(\mathbf{X}, \mathbf{y}) = r(\hat{\mathbf{y}}, \mathbf{y}) = \frac{\hat{\mathbf{y}}_c^\top \mathbf{y}_c}{\sqrt{\hat{\mathbf{y}}_c^\top \hat{\mathbf{y}}_c} \sqrt{\mathbf{y}_c^\top \mathbf{y}_c}} \quad (1)$$

where,

$$\hat{\mathbf{y}} = \mathbf{X}^* \boldsymbol{\beta}, \quad \text{s.t. } \mathbf{X}^* = [\mathbf{1}, \mathbf{X}] \quad (2)$$

$\hat{\mathbf{y}}$ refers to a vector containing the predicted values of the label. \top indicates the matrix transpose. Subscript c means the variables are centralised. \mathbf{X}^* is an augmented matrix of dimension $N \times (n + 1)$. $\boldsymbol{\beta}$ can be obtained from the normal equations for a linear multiple regression with a least-squares cost function, which can be written as,

$$\boldsymbol{\beta} = (\mathbf{X}^{*\top} \mathbf{X}^*)^{-1} \mathbf{X}^{*\top} \mathbf{y} \quad (3)$$

The MCC is a scalar, taking values from 0 to 1. A sensor combination corresponding to a higher MCC value indicates that the features from these sensors may perform better when predicting the labels. The cost function defined by the MCC is an efficient means of searching for the optimal spatial deployment of sensors with different numbers.

Note that the labels can usually be represented by a vector, but it may happen that the labels are represented by a matrix, for example, when the labels should be dummy encoded to a matrix to avoid adding order information. In this case, the *canonical correlation coefficient* can be adopted to replace the MCC. However, there is no research to theoretically prove which encoding method can make the selected features better predict the labels in the model training step. Furthermore, considering computational efficiency, the MCC is selected as an example in this paper. It is suggested that the criterion applied at this stage can be any criterion used in filter methods for feature selection, which measure the relevance of features from sensors by their correlation with dependent variables, without actually training a model on features.

Stage 2 - optimal sensor number and type

For the final design stage of a sensor system, the assessment criteria are composed of parameters or derivations of the confusion matrix, allowing the intuitive consideration of the SHM system's performance. Based on the characteristics of the feature set distribution, the purpose of classification and the consequences of misclassification, an appropriate criterion can be selected for the second stage of a system design. The parameters of the confusion matrix are demonstrated in Table I.

The results based on these criteria are related to the selected type of classifier. Therefore, at this stage, it is necessary to determine the possible classifiers which will be used

TABLE I. Terminology in a confusion matrix.

		Measured condition	
		Positive	Negative
Predicted condition	Positive	True positive (tp)	False positive (fp)
	Negative	False negative (fn)	True negative (tn)

P refers to positive; N refers to negative

for classifying the data once the structure is put into use. Since the number of optimal sensor combinations with different sensor numbers and sensor types is expected to be relatively small at this stage thanks to the optimisation conducted in Stage 1, it is feasible to train the associated classifiers and compare them with each other.

For binary classification, the receiver operator characteristic (ROC) curve is a commonly-used criterion to indicate the diagnostic ability of an classification system. The ROC curve consists of true positive rate and false positive rate. The area under the curve (AUC) makes it easy to compare one ROC curve to another. Thus, AUC is a criterion considered in the sensor system evaluation step for the cases of binary classification.

For multiclass classification, a derivation from the confusion matrix, accuracy, is taken as an example to assess system performance. A higher accuracy means a better decision can be made by the established SHM system. Overall accuracy can be calculated from the confusion matrix by,

$$Accuracy = \frac{tp + tn}{tp + tn + fp + fn} \quad (4)$$

The variables in this equation are defined in Table I.

A NUMERICAL CASE STUDY

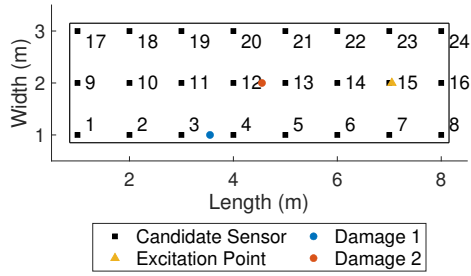
A state-space model of a plate structure with 24 degrees of freedom (DoFs) is used for demonstration in this paper with the simulation carried out in MATLAB version R2018b. The parameters of the 24 DoF model are given in Table II. Each lumped-mass node provides a candidate location for the sensor, as demonstrated in Figure 1a. The simulated boundary condition is fixed-free. Figure 1b shows the first four mode shapes of this structure.

Observations of this structure are simulated by using the state-space model to acquire time-series data and then via the Fourier transform to obtain the frequency response functions (FRFs). A white noise Gaussian excitation is employed as the input force. Noise with a prescribed signal-to-noise ratio (SNR) is introduced into the simulated time-series data to represent the noise effects corresponding to different sensor types. Note that the type of sensor is characterised by the SNR. There is a rule of thumb that the higher the sensor cost, the higher the SNR of data. Four SNRs ranging from 45dB to 30dB (with an interval of 5dB) are adopted here to simulate four sensor types. They are high-precision sensors, medium-precision sensors, low-precision sensors, and extremely low-precision sensors respectively.

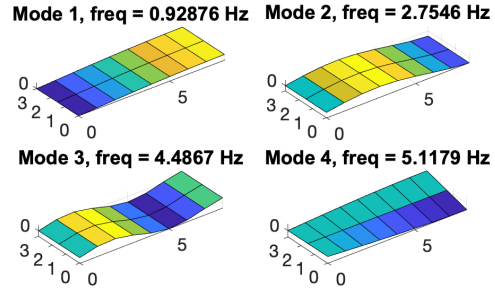
TABLE II. The parameters of the plate structure.

Parameter	Mean (μ)	SD (σ)	Distribution
m, kg	1	0	N/A
k, N/m	1000	30	Normal (independent)
c, N/(m/s)	1	0.03	Normal (dependent on k)
Damage 1, N/m	200	0	N/A
Damage 2, N/m	200	0	N/A

m: Mass; k: Stiffness; c: Damping



(a) Labels for simulated conditions.



(b) First 4 mode shapes.

Figure 1. Schematic of the simulated 2-D plate and the corresponding mode shapes.

This approach was used to provide predicted normal condition data and damaged-state data for the design stage of an SHM system. In a practical setting, the damage cases of interest would be determined by failure mode and effect analysis. In this case study, damage is simulated by reducing the local stiffness. The position and extent of the simulated damage can be changed according to the research needs. Two damage cases are considered in this case study by reducing the stiffness value at two positions by 200 N/m, which is included in Table II. The positions of the damage are shown in Figure 1a.

Uncertainty analysis

The focus of this paper is not on how to provide reliable data sets, so here the introduction of uncertainty in the stiffness parameters is a simple example of how to consider the discordance between the FE model and the real structure. Because proportional damping dependent on stiffness was used in this simulation, an uncertain damping effect was also involved. Other parameters related to material properties or geometry were held constant. The mean values and standard deviations of the uncertain parameters of the 24-DoF model are given in Table II.

Latin hypercube sampling (LHS) was adopted to efficiently generate the random samples of the uncertain parameters. After partitioning a cumulative curve into N intervals with the equal cumulative probability, LHS proceeds by randomly selecting one sample from each interval. The convergence of mean value and standard deviation of the first three natural frequencies for different sample sizes was used to determine the required sample size, as shown in Figure 2. It was found that both indicators remained stable after 150 samples; thus, 150 was selected as the number of samples. After obtaining 150 samples of this plate structure in the healthy state, 150 samples for two damage cases were obtained respectively by reducing the stiffness at the position of damage 1 or damage 2.

In addition to the parametric uncertainty, the uncertainty caused by the influence of noise on the time series data was also taken into account. For each model sample, 20 time-series observations were simulated under each specified signal-to-noise ratio to consider the effect of noise. Therefore, 3000 measurements are available for each of the normal state, damaged state 1 and damaged state 2 in the case study.

Sensor placement optimisation

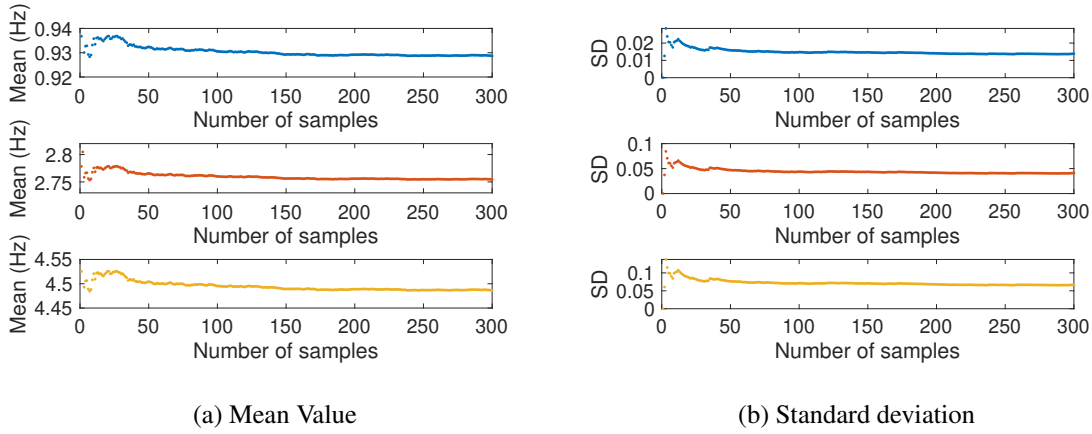


Figure 2. Mean value and standard deviation for the first three natural frequencies of model samples.

Before conducting SPO, effective features should be extracted from the output signals of all candidate sensors. One option for generating robust features using FRFs is the multivariate outlier analysis approach introduced in [10]. Here, a frequency range (FR) with a specific resolution can be selected to generate features by using the Mahalanobis squared-distance (MSD) technique to compute the discordance between an observation and a training set. The equation to calculate MSD-based features is as follows:

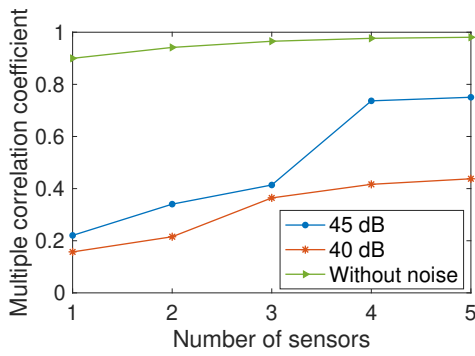
$$D_M^2 = (\mathbf{x} - \bar{\boldsymbol{\mu}})^\top \mathbf{S}^{-1} (\mathbf{x} - \bar{\boldsymbol{\mu}}) \quad (5)$$

where \mathbf{x} is a vector referring to an observation, $\bar{\boldsymbol{\mu}}$ and \mathbf{S} are the mean value and covariance matrix for a set of baseline observations respectively. \top indicates transpose.

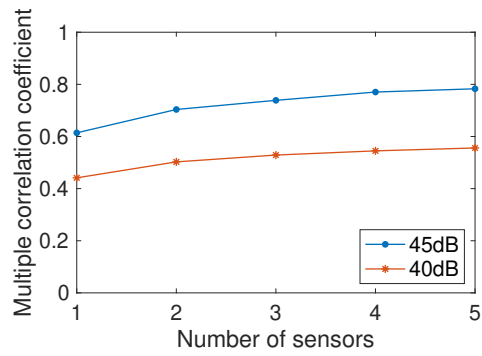
This kind of feature can naturally account for uncertainty effects in the case that the normal condition data includes measurements under different conditions, designed to be filtered out [11]. Therefore, the normal condition data for 150 random samples of the plate structure were used to calculate the mean value and the covariance required in equation 5.

By comparing the averaged FRFs of the 150 samples for the normal condition and two damaged states separately, the third peak and its vicinity of the FRFs (frequency range between 4.3 Hz and 4.7 Hz) were selected to generate MSD-based features, in which range the normal state data and the damaged state data are more distinguishable.

In order to provide an upper bound on performance, an exhaustive search was utilised to search out the optimal deployment of sensors with different numbers of sensors. The cost function (or fitness function) was constructed by the MCC. The preferred classification algorithm here to facilitate the final system evaluation is a linear support vector machine (SVM), since it is simple and makes no assumption about the data distribution. The hyperparameters of this algorithm are optimised by minimising five-fold cross-validation loss. When the type of sensor changes, the same optimisation process was repeated.



(a) Data set involving uncertainty.



(b) Data set involving uncertainty and noise.

Figure 3. Results of SPO based on different data sets.

RESULTS AND DISCUSSION

The effect of noise on optimisation

To evaluate whether it is necessary to consider the noise effect in the optimisation process, a set of comparisons based on damage case 2 are made here. The effectiveness of a sensor combination is assessed via the MCC.

At first, MSD-based features of 150 sampling models were used to decide a group of optimal sensor combinations with different numbers of sensors. These features only included the influence of uncertain model parameters. The optimal MCC values calculated by using these 300 features (150 normal condition features and 150 damaged state features) are plotted in Figure 3a, marked in green. The corresponding optimal sensor combinations determined at the previous step were then applied to calculate the MCC values for features extracted from sensor networks with two different SNRs (45 dB and 40 dB) (See Figure 3a for the results).

In contrast, the other two groups of optimal sensor combinations with different number of sensors were obtained by directly using features involving both parametric uncertainties and noise with different levels (including 45 dB and 40 dB). The corresponding results are shown in Figure 3b.

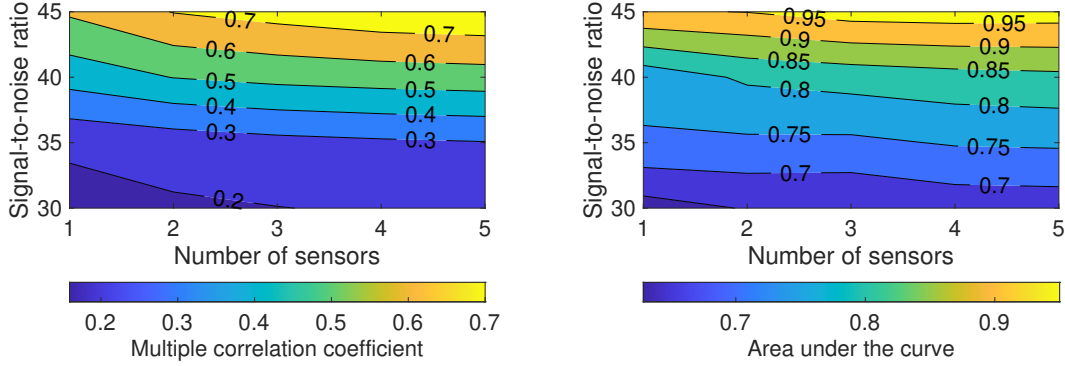
By comparing the results in the above two figures, it can be seen that the MCC values in Figure 3a for two conditions with different SNRs are always smaller than the MCC values in Figure 3b for the same two conditions. Thus, the SPO using features only involving parametric uncertainties can not provide optimal results when the background noise is considered in the simulation of sensor outputs. This result indicates that, as expected, the noise has a significant impact on the result of optimisation. Therefore, at the design stage of a sensor system, the influence of noise should be incorporated into the optimisation process.

Sensor placement optimisation for binary classification

The normal condition and second damage case were taken as an example to carry out the SPO for a binary classification. For four situations with different SNRs, an

TABLE III. Optimal sensor combinations for the detection of damage 2.

Num. of sensors	Signal-to-noise ratio			
	45 dB	40 dB	35 dB	30 dB
1	12	11	9	1
2	12,14	9,11	9,16	1,16
3	9,12,14	9,11,17	9,15,16	1,15,16
4	5,10,12,14	1,9,11,17	9,15,16,20	1,8,15,16
5	5,6,10,12,14	1,9,11,17,18	5,9,15,16,22	1,8,12,15,16



(a) Contour plot of MCC.

(b) Contour plot of AUC.

Figure 4. Two types of contour plots for binary classification.

exhaustive search was used to find the optimal sensor combination with the number of sensors ranging from 1 to 5. The optimal results are presented in Table III, and the corresponding MCC values can be referred to in Figure 4a. The locations of sensors are as indicated in Figure 1a. It can be seen that as the SNR decreases, the distribution of sensors moves from the nodes centred on the damage 2 location to the nodes providing high-amplitude signals.

After determining the optimal sensor combinations with different numbers of sensors, the ROC curves for these optimal sensor networks can be calculated to finally decide the type and number of sensors to be installed. To compare these curves conveniently, the values of AUC are calculated and plotted in Figure 4b.

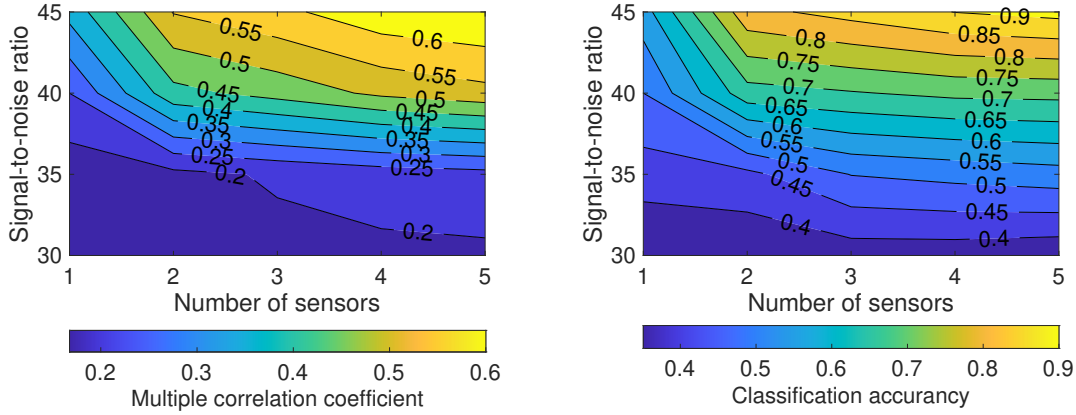
Figures 4a, 4b indicates that those sensor combinations with higher MCC values have a higher AUC. Therefore, it is reasonable to use MCC as a criterion to effectively determine the spatial combination of sensors. However, MCC values can not reflect the performance of a established sensor system intuitively. Therefore, it is necessary to calculate the ROC curve and AUC value via the selected classification algorithm to facilitate the final decision on whether or not to implement the system.

Sensor placement optimisation for multiclass classification

The optimal spatial distributions of sensors for detecting damage cases 1 and 2 are presented in Table IV and the optimal objective function values (MCC) are shown in Figure 5a. For this multiclass classification task, the selected sensor distribution was

TABLE IV. Optimal sensor combinations for the detection of damage 1 and 2.

Num. of sensors	Signal-to-noise ratio			
	45 dB	40 dB	35 dB	30 dB
1	2	1	3	3
2	2,18	1,13	3,15	3,15
3	1,2,18	1,2,13	1,3,18	3,4,15
4	1,2,14,17	1,2,5,13	1,3,15,18	3,4,12,15
5	1,2,6,14,17	1,2,5,12,13	1,3,5,15,18	3,4,6,15,18



(a) Contour plot of MCC.

(b) Contour plot of accuracy.

Figure 5. Two types of contour plots for multiclass classification.

found to exhibit the following phenomenon. When the introduced SNR is high, the selected sensors will be respectively distributed around the two areas centred on the two damaged locations. As the noise level increases (SNR decreases), the distance between these two areas becomes smaller. The 5-fold cross-validation classification accuracy of the SHM systems composed of these optimal sensor networks is calculated and plotted in Figure 5b.

As shown in Figures 5a, 5b, the contour plots of MCC and accuracy achieved by the fully-trained classifier exhibit similar trends across the number of sensors and sensor accuracy. Therefore, it is deemed practical to use MCC as a low-cost criterion for the multiclass classification to decide a spatial sensor deployment.

Performance comparison of assessment criteria for two stages

In order to quantitatively measure the damage detection performance of the sensors selected by MCC and the efficiency of the MCC as the selection criteria, a set of comparisons are made here. First, the accuracy is directly used as the criterion to search out the optimal sensor combinations. In order to reduce the hyperparameter optimisation time to make it possible to calculate the accuracy of all possible sensor combinations, each model sample under one noise level uses only four measurements to construct a data set used here. Therefore, the number of measurements for the normal state, the damaged state 1 and the damaged state 2 are 600 respectively. One- and two-sensor location(s)

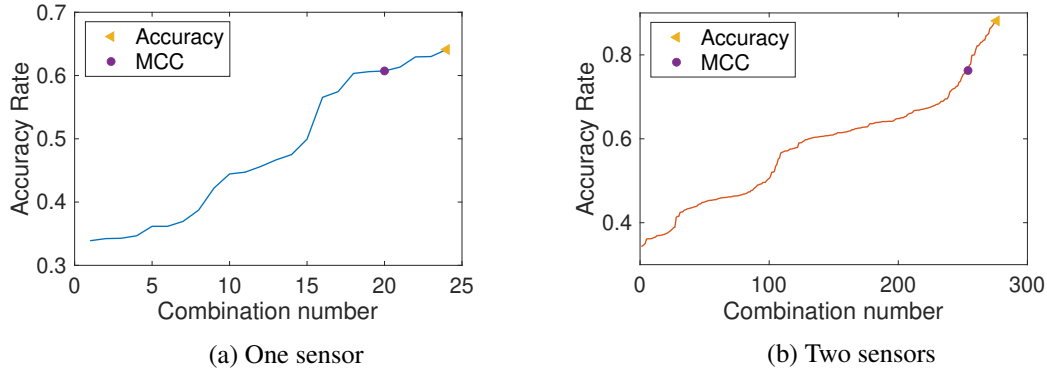


Figure 6. Sorting accuracy and optimal results of two assessment criteria.

TABLE V. Optimal results and calculation time for the two assessment criteria.

Criterion	Num. of sensors			
	1	Time (s)	2	Time (s)
Accuracy	9	5.82×10^3	2,12	2.00×10^5
MCC	2	0.37	2,19	1.11

are selected from 24 candidates. The considered SNR is 45 dB. At this noise level, the accuracy of all possible sensor combinations is shown in Figure 6, and arranged in ascending order. The optimal results are presented in Table V.

On the contrary, for the same data set, the accuracy values of the best sensor combinations determined based on the MCC are calculated, and the optimal results are given in Table V and Figure 6. It can be seen that the accuracy of the optimal sensor combination received by MCC is close to the best result received by directly using accuracy as the objective function. However, the calculation time corresponding to the MCC-based optimisation is greatly reduced. Therefore, in practical application, the MCC-based criterion can be applied to reduce the number of combinations, and accuracy can further refine the selection of sensor combinations with different sensor numbers and sensor types.

CONCLUSIONS

In this paper, a systematic framework for sensor system design combined with a classification algorithm is established. The parametric uncertainty and background noise are involved in the optimisation process to consider the discrepancy between numerical simulation and the real situation.

The main contribution of this paper is to divide the SPO into two steps, including selecting the best sensor combination and determining the number of sensors and sensor types, and at the same time, proposing appropriate evaluation criteria for each step. A case study of a plate structure is carried out. The results indicate that the proposed assessment system greatly improves the speed of sensor-system design while considering the detection performance of the designed sensor system.

REFERENCES

1. Choi, S.-K., R. Grandhi, and R. A. Canfield. 2006. *Reliability-based Structural Design*, Springer Science & Business Media, London, UK.
2. Smith, R. C. 2013. *Uncertainty Quantification: Theory, Implementation, and Applications*, vol. 12, Siam, Philadelphia, USA.
3. Imamura, T., W. C. Meecham, and A. Siegel. 1965. "Symbolic calculus of the Wiener process and Wiener-Hermite functionals," *J MATH PHYS*, 6(5):695–706.
4. Kennedy, M. C. and A. O'Hagan. 2001. "Bayesian calibration of computer models," *J ROY STAT SOC B*, 63(3):425–464.
5. Haykin, S. and R. Lippmann. 1994. "Neural networks, a comprehensive foundation," *INT J NEURAL SYST*, 5(4):363–364.
6. Guratzsch, R. F. and S. Mahadevan. 2010. "Structural health monitoring sensor placement optimization under uncertainty," *AIAA J*, 48(7):1281–1289.
7. Castro-Triguero, R., S. Murugan, R. Gallego, and M. I. Friswell. 2013. "Robustness of optimal sensor placement under parametric uncertainty," *MECH SYST SIGNAL PR*, 41(1-2):268–287.
8. Eshghi, A. T., S. Lee, H. Jung, and P. Wang. 2019. "Design of structural monitoring sensor network using surrogate modeling of stochastic sensor signal," *MECH SYST SIGNAL PR*, 133, doi:10.1016/j.ymsp.2019.106280.
9. Allison, P. D. 1999. *Multiple Regression: A Primer*, Pine Forge Press Inc., California, USA.
10. Manson, G., K. Worden, and D. Allman. 2003. "Experimental validation of a structural health monitoring methodology: Part III. Damage location on an aircraft wing," *J SOUND VIB*, 259(2):365–385.
11. Deraemaeker, A. and K. Worden. 2018. "A comparison of linear approaches to filter out environmental effects in structural health monitoring," *MECH SYST SIGNAL PR*, 105:1–15.